

Improved Solution Approach for Aerodynamics Loads of Helicopter Rotor Blade in Forward Flight

Aleksandar Bengin¹ - Časlav Mitrović¹ - Dragan Cvetković*² - Dragoljub Bekrić¹ - Slavko Pešić¹

¹University of Belgrade, Faculty of Mechanical Engineering, Serbia

²University "Singidunum" Belgrade, Faculty of Business Information Science, Serbia

This paper presents the numerical model developed for rotor blade aerodynamics loads calculation. The model is unsteady and fully three-dimensional. Helicopter blade is assumed to be rigid, and its motion during rotation is modeled in the manner that rotor presents a model of rotor of helicopter Aerospatiale SA 341 "Gazelle" (the blade is attached to the hub by flap, pitch and pseudo lead-lag hinges). Flow field around the blade is observed in succession of several azimuth locations. Flow field around helicopter rotor is modeled as fully three-dimensional, unsteady and potential. Blade aerodynamics is modeled using a lifting surface model. Rotor wake is generated from the straight elements of constant vorticity, released from the trailing edge, at fixed azimuth angles. These vortices represent both trailed and shed wake components, and are allowed to freely convect along local velocity vectors. Wake is modeled as free one, and its shape at certain moment can be calculated from simple kinematics laws applied on collocation points of the wake. Wake distortion is calculated only in the rotor near-field, i.e. in finite number of rotor revolutions. Vortex elements are modeled with vortex core. The radius of the vortex core is assumed independent of time, and it depends on circulation gradient at the point of vortex element released from the blade.

© 2008 Journal of Mechanical Engineering. All rights reserved.

Keywords: unsteady aerodynamics, helicopter rotor blade, potential flow, lifting surface theory

0 INTRODUCTION

One of the most important challenges in helicopter aerodynamics is the accurate prediction of rotor loads, especially in forward flight.

Helicopter rotor aerodynamic flow field is very complex, and it is characterized by remarkably unsteady behavior. The most significant unsteadiness appears during the forward flight. In that case, the progressive motion of helicopter coupled with rotary motion of rotor blades causes drastic variations of local velocity vectors over the blades, where the advancing or retreating blade position is of great significance. In first case, the local tip transonic flow generates, while in second, speed reversal appears.

In addition, in forward flight, blades encounter wakes generated by forerunning blades and so encounter non-uniform inflow. The wake passing by the blade induces high velocities close to it causes changes in lifting force. Besides that, in horizontal flight blades constantly change pitch, i.e. angle of attack at different azimuths. Such angle of attack variations are very rapid, so that dynamic

stall occurs, especially in case of retreating blades [1] and [2].

Various methods have been used to represent the rotor and its wake. The rotor blades have been represented by actuator disc, blade elements, a lifting line, lifting surface, or a finite difference and finite elements method. Lifting surface theory allows for a more realistic and general representation of the blade than lifting line theory, and has been shown to be more accurate as well [2] to [4]. Finite difference or finite element methods must be used to introduce transonic effect. Also, they offer the potential to predict blade drag [5]. However, the major drawback of finite elements and finite difference methods are their long computation times.

1 DYNAMICS

In this paper the rotor of helicopter SA 341 "Gazelle" is modeled, at which the blades are attached to the hub by flap, pitch and pseudo lead-lag hinges.

Blade motion in lead-lag plane is limited by dynamic damper, which permits very small

*Corr. Author's Address: University "Singidunum", Faculty of Business Information Science, Danijelova St. 32, 11000 Belgrade, Serbia, dcvetkovic@singidunum.ac.yu

maximum blade deflection. Due to such small angular freedom of motion, we can assume that there is no led-lag motion at all.

Pitch hinge is placed between flap hinge and pseudo lead-lag hinge. In derivation of the equations of motion [6] and [7], the following was assumed:

- the rotor does not vibrate, and its rotation velocity Ω is constant,
- the blade is considered absolutely rigid.

According to the above mentioned, the following frames have been selected for use:

- fixed frame F, with x -axis in the direction of flight, and z -axis oriented upwards;
- frame H, connected with the rotor and rotates together with it; it is obtained by rotating the F frame for a certain azimuth angle ψ ; keeping the common z -axis;
- frame P, connected to the flapping hinge, so that the y -axis is oriented along the blade; its origin is displaced from the rotating axis for the value e_p , while it is rotated for the angle β with respect to the frame H;
- frame B, connected to the blade, displaced for the value e_b from the origin of P, and tilted for the value θ (pitch angle) with respect to the P.

With assumptions mentioned above, equation of blade flapping motion is [7]:

$$B\ddot{\beta} + \Omega^2 (B \cos \beta + m_b e_b x_g R) \sin \beta = M_A$$

where B is moment of inertia about P_x , m_b mass of the blade, x_g position of blade center of gravity in P frame, and M_A is aerodynamic moment.

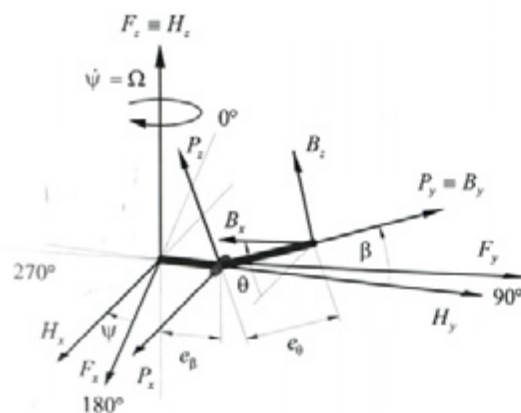


Fig. 1. Coordinate systems

2 AERODYNAMICS

2.1 Analytical Model

The flow field is assumed to be potential (inviscid and irrotational) and incompressible. In that case, velocity potential satisfies the Laplace equation:

$$\Delta \Phi = 0$$

The equation is the same, both for steady and unsteady flows. Owing to that, methods for steady cases can be applied for the solution of unsteady flow problems, as well. Unsteadiness is introduced by unsteady boundary condition:

$$(\vec{v} - \vec{v}_T) \cdot \vec{n} = 0$$

of the Kelvin theorem:

$$\frac{d\vec{\Gamma}}{dt} = 0$$

and the unsteady form of the Bernoulli equation:

$$\frac{p - p_\infty}{\rho_\infty} = V_\infty^2 - V^2 - 2 \frac{\partial \Phi}{\partial t}$$

In order to define the aerodynamic characteristics of blades, two models should be established: blade model and wake model.

The blade is modeled as a thin lifting surface, which enables a complete 3D modeling around helicopter blades. Lifting surface model is more accurate in the treatment of the 3D effects at low angle of attack, and with some extensions, compressible flow effects. It is very suitable for modeling any blade geometry (symmetrical or non-symmetrical airfoils, various blade shape, blade tips i.e.), since they do not need airfoil experimental data. Unfortunately, it cannot deal with viscous flows, and thus is no more accurate than lifting line theory at high angle of attack.

Numerical modeling of the wake must be done very carefully due to its high influence on the lift force generation. The free-wake model, which is applied in this paper, is one of the most advanced, since it can cover all relevant problems connected with the wake influence.

2.2 Unsteady Kutta Condition

In case of inviscid problems, it is necessary to satisfy Kutta condition at the trailing edge [8] to [10].

Based on unsteady Bernoulli equation, the pressure coefficient for unsteady flow is defined as:

$$C_p = \frac{p - p_\infty}{\frac{1}{2} \rho_\infty V_\infty^2} = 1 - \frac{V^2}{V_\infty^2} - \frac{2}{V_\infty^2} \frac{\partial \Phi}{\partial t}$$

According to that, the difference between upper and lower surface pressure coefficients is:

$$\Delta C_p = C_{p_u} - C_{p_l} = -\frac{V_U^2 - V_L^2}{V_\infty^2} - \frac{2}{V_\infty^2} \frac{\partial}{\partial t} (\Phi_U - \Phi_L) \quad (1),$$

where subscripts U and L denote upper and lower surface values.

In case of the thin lifting surface, with the assumption that spanwise velocity components are small, the potential difference can be written as an integral from leading edge to a certain point M at the surface:

$$\Phi_U - \Phi_L = \int_{LE}^M (V_{U_t} - V_{L_t}) dl$$

where the tangential velocity difference is the local bound vortex distribution:

$$\gamma = (V_{U_t} - V_{L_t})$$

Final equation defining the potential difference is:

$$\Phi_U - \Phi_L = \int_{LE}^M \gamma dl \quad (2).$$

If we assume that spanwise velocities are small, the difference of velocity squares can be calculated as:

$$V_U^2 - V_L^2 \approx 2V_\infty \gamma \quad (3).$$

By substituting (3) and (2) in (1), the following equation is obtained:

$$\Delta C_p = -\frac{2}{V_\infty^2} \left(V_\infty \gamma + \frac{\partial}{\partial t} \int_{LE}^M \gamma dl \right)$$

The Kutta condition can be expressed as the uniqueness of pressure coefficients at the trailing edge, which, mathematically expressed, takes the form:

$$\Delta C_p = -\frac{2}{V_\infty^2} \left(V_\infty \gamma_{TE} + \frac{\partial}{\partial t} \int_{LE}^{TE} \gamma dl \right) = 0$$

Since it is impossible to be $V_\infty = \infty$, the relation within the parentheses must be equal to zero:

$$V_\infty \gamma_{TE} + \frac{\partial}{\partial t} \int_{LE}^{TE} \gamma dl = 0 \quad (4).$$

The integral in the upper equation is, in fact, the contour circulation, which covers the lifting surface:

$$\tilde{\Gamma} = \int_{LE}^{TE} \gamma dl$$

so, the equation (4) can be written as:

$$V_\infty \gamma_{TE} + \frac{\partial \tilde{\Gamma}}{\partial t} = 0$$

The expression for unsteady Kutta condition comes out directly as [11] and [12]:

$$\frac{\partial \tilde{\Gamma}}{\partial t} = -V_\infty \gamma_{TE}$$

If the right hand-side part is substituted with (3) written for the trailing edge, we obtain:

$$\frac{\partial \tilde{\Gamma}}{\partial t} = -\frac{V_{U_{te}}^2 - V_{L_{te}}^2}{2} = -(V_{U_{te}} - V_{L_{te}}) \frac{V_{U_{te}} + V_{L_{te}}}{2}$$

From this equation, it can be clearly seen that the variation of the lifting surface circulation in time can be compensated by releasing vortices of magnitude $(V_{U_{te}} - V_{L_{te}})$ at the velocity $(V_{U_{te}} + V_{L_{te}})/2$.

3 DISCRETIZATION AND NUMERICAL SOLUTION PROCEDURE

The method for the solution of this problem is based on the coupling of the dynamic equations of blade motion with the equations of aerodynamics. It is not possible to obtain an analytical solution of this problem, so discretization and numerical approach must be accepted.

Discretization in time is done by observing the flow around the blade in a series of positions that it takes at certain times $t_k (k = 0, 1, 2, \dots)$, which are spaced by finite time intervals Δt at different azimuths.

Discretization of the thin lifting surface is done by using the panel approach [12] and [13]. By this method, the lifting surface is divided in a finite number of quadrilateral surfaces – panels. Vorticity distribution is discretized in a finite number of concentrated, closed quadrilateral linear vortices, whose number is equal to the number of panels, in such a way that one side of the linear vortex is placed at the first quarter chord of the panel, and represents the bound vortex of the corresponding panel. The opposite side of the vortex is always placed at the trailing edge, while the other two sides are parallel to the flow. The wake is represented by quadrilateral vortex in the

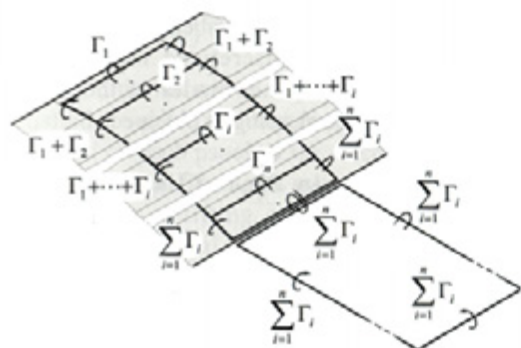


Fig. 2. The steady panel scheme

airflow behind the lifting surface. One side of it is connected to the trailing edge, while the opposite one is at the infinity. The other two sides (trailing vortices), which actually represent the wake, are placed parallel to the airflow. The vorticity of the quadrilateral vortex is equal to the sum of the vorticities of all bound vortices of the panels that correspond a certain lifting surface chord, but opposite in direction. Then the trailing edge vorticity is equal to zero.

Model established in such a manner corresponds to the steady flow case. On the other hand, it can be very easily spread in order to include the unsteady effects.

3.1 Vortex Releasing Model

The variation of the lifting surface position in time induces variation of circulation around the lifting surface as well. According to the Kelvin theorem, this variation in circulation must also induce the variation around the wake. According to the unsteady Kutta condition, this can be achieved by successive releasing of the vortices in the airflow [13].

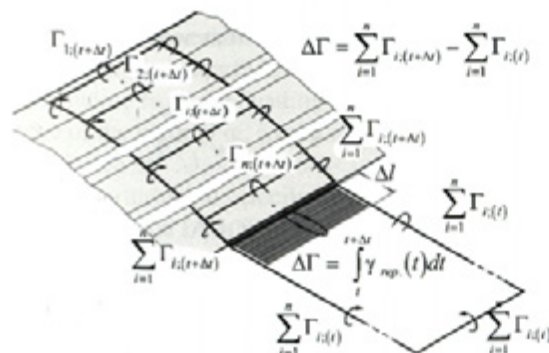


Fig. 3. Vortex releasing

Suppose that the lifting surface has been at rest until the moment t , when it started with the relative motion with respect to the undisturbed airflow. The vortex releasing, as a way of circulation balancing, is done continuously, and in such a way a vortex surface of intensity $\gamma(t)$ is formed.

At the next moment $t + \Delta t$, the flow model will look like in Fig. 3. The circulation of the vortex element joined to the trailing edges equal to the difference in circulations at moments $t + \Delta t$ and t . We will discretize the vortex "tail" by replacing it with the quadrilateral vortex loop, whose one side is at the trailing edge, and the opposite side is at the finite distance from the trailing edge (shed vortex). By this, we can obtain the final model for unsteady case.

3.2 Discretization of Wake

The established vortex-releasing model is appropriate for the wake modeling using the "free wake" approach [13] to [15].

During the time, by continuous releasing of the quadrilateral vortex loops, the vortex lattice formed of linear trailed and shed vortices is created. The collocation points of the vortex lattice are node points. The wake distortion is achieved by altering the positions of the collocation points in time, by application of a rather simple kinematics relation:

$$\vec{r}_i(t + \Delta t) = \vec{r}_i(t) + \vec{V}_i(t)\Delta t$$

The velocities of the collocation points are obtained as sums of the undisturbed flow velocity and velocities induced by other vortex elements of the flow field.

Induced velocities are calculated using the Biot-Savart law. In order to avoid the problems of

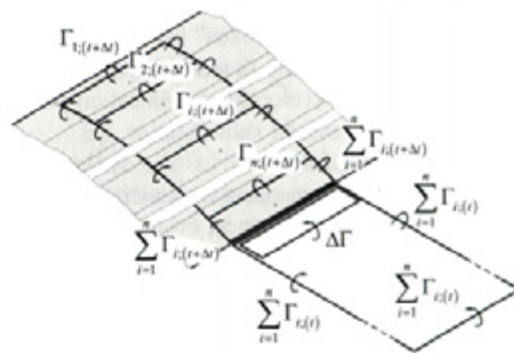


Fig. 4. Unsteady panel scheme

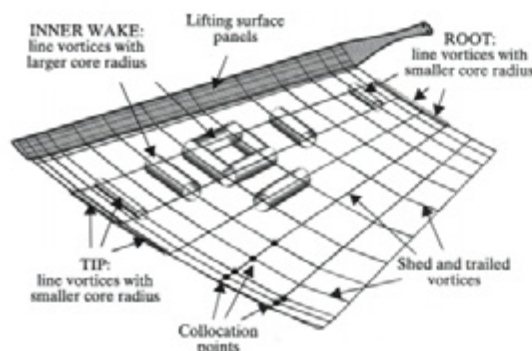


Fig. 5. Discretized wake

velocity singularities, line vortex elements are modeled with viscous core. The existence of the vortex core has remarkable influence in blade-wake interactions, since in this way large velocity irregularities on the blade close to the wake are avoided. Thus, using appropriate core model is important for accurate predictions of the wake development. Distributed core model is used since it is more realistic [1].

The core radius varies with the gradient of the bound circulation at the position where vortex is released, from the value $r_c = 0.00275R$ (where R is the rotor diameter) for the elements at the end of the wake (high gradient positions), to the values $r_c = 0.05R$ inside the wake (low gradients) [16].

The wake influence at large distances from the blade is negligible, so it is possible to neglect the wake distortion at a sufficient distance from the rotor. The area in which distortion is relevant depends on the helicopter flight regime, and it can be determined by the advance ratio μ [1]:

$$m = \frac{0.4}{\mu}$$

where m is the number of revolutions for which it is necessary to calculate the wake distortion. After that, the wake shape is "frozen" in achieved state, and it moves through the flow field keeping it for the rest of the time (velocity of collocation points is equal to the flow field velocity).

The "frozen" part of the wake still influences the adjacent area in which it is still being distorted. After some distance, even the influence of the "frozen" part becomes negligible, and then it is eliminated from the model. Decision of elimination row of shed and trail vortex elements from "frozen" part of the wake is made when the intensity of velocities they induced on blade panels

becomes smaller than prescribed value close to zero. In this way, a discretized wake model, consistent with the panel model of the lifting surface and vortex releasing is obtained.

3.3 Discretization in Time of Unsteady Kutta Condition

Let us consider the unsteady Kutta condition from the aspect of the assumed discretized model. The condition can be written as:

$$V_\infty \gamma_{TE} + \frac{\partial \tilde{\Gamma}}{\partial t} = 0 \quad (5)$$

In case of transition to the discretized time domain, it is necessary to substitute the partial derivative with the finite difference form:

$$\frac{\partial \tilde{\Gamma}}{\partial t} = \frac{\tilde{\Gamma}(t + \Delta t) - \tilde{\Gamma}(t)}{\Delta t} = \frac{\Delta \tilde{\Gamma}}{\Delta t}$$

By substituting this equation in (5), we obtain:

$$V_\infty \gamma_{TE} + \frac{\tilde{\Gamma}(t + \Delta t) - \tilde{\Gamma}(t)}{\Delta t} = 0 \quad (6)$$

In case of numerical solutions, it is customary to satisfy Kutta condition in vicinity of the trailing edge. According to that, the intensity of the distributed vorticity at the trailing edge γ_{TE} is treated as equal to the intensity of the distributed vorticity at the trailing edge panel γ_n . The intensity of the distributed vorticity is constant at every panel, so it can be written:

$$\gamma_{TE} = \gamma_n = \frac{\Gamma_n}{l_n}$$

where γ_n is intensity of the distributed vorticity at the trailing edge panel, and l_n is the panel cord length. Substituting this equation in (6), we have:

$$V_\infty \frac{\Gamma_n}{l_n} + \frac{\tilde{\Gamma}(t + \Delta t) - \tilde{\Gamma}(t)}{\Delta t} = 0$$

i.e. the difference of circulations around the lifting surface at the moments $t + \Delta t$ and t can be calculated by:

$$\tilde{\Gamma}(t + \Delta t) - \tilde{\Gamma}(t) = -V_\infty \frac{\Gamma_n}{l_n} \Delta t$$

4 DEFINITION OF EQUATION SET

The boundary condition of impermeability of the lifting surface should be satisfied at any moment of time, $t_k (k = 0, 1, 2, \dots)$ in a finite number of points of lifting surface:

$$(\vec{V}_i - \vec{V}_{Ti}) \cdot \vec{n}_i = 0; \quad i = 1, 2, \dots, N$$

Points at which this condition must be satisfied are called the control points. One of them is placed on each panel, at the three-quarter chord panel positions. By this, at every moment of time, the number of lifting surface impermeability conditions is equal to the number of unknown values of circulations of bound vortices.

The equations of motion of the lifting surface are known, as well as the velocities \vec{V}_{Ti} of all characteristic points, and their normals \vec{n}_i as well.

At each flow field point, velocity can be divided to the free stream velocity and perturbation velocity:

$$\vec{V}_i = \vec{V}_\infty + \vec{w}_i$$

The perturbation velocity is induced by lifting surface and wake vortex elements. Boundary condition of impermeability of the lifting surface can be written at any moment of time as:

$$(\vec{V}_\infty + (\vec{w}_i)_B + (\vec{w}_i)_S + (\vec{w}_i)_W - \vec{V}_{Ti}) \cdot \vec{n}_i = 0 \quad (7),$$

where perturbation velocities are:

$(\vec{w}_i)_B$ – induced by bound vortices,

$(\vec{w}_i)_S$ – induced by shed vortices,

$(\vec{w}_i)_W$ – induced by wake vortices.

At every moment, the wake shape and circulations of its vortex lines are known, and so the wake-induced velocity at every flow field point is known as well. On the other hand, the circulations of the bound vortices are unknowns (their positions are defined by the lifting surface shape).

Therefore, equation (7) can be rewritten in the form where unknowns are on the left side, and knowns are on the right side of the equation (fact is that second term on the left side has an unknown and a known part, as will be shown later):

$$(\vec{w}_i)_B \cdot \vec{n}_i + (\vec{w}_i)_S \cdot \vec{n}_i = (\vec{V}_{Ti} - \vec{V}_\infty) \cdot \vec{n}_i - (\vec{w}_i)_W \cdot \vec{n}_i \quad (8).$$

Let us consider one column of the n panels on the lifting surface which spreads itself chordwise, from the leading edge to the trailing edge of the blade (Fig. 6) and shed vortex AD with circulation $\Delta\tilde{\Gamma}$.

Perturbation velocity in the first term on the left side of the equation (8) can be calculated as sum of the velocities induced by bound vortices:

$$(\vec{w}_i)_B = \sum_{j=1}^n (\vec{w}_{i,j})_B$$

where $(\vec{w}_{i,j})_B$ is velocity induced by j -th bound vortex.

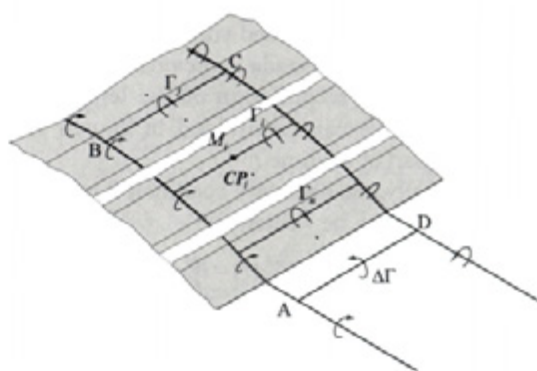


Fig. 6. One chordwise column of panels on the lifting surface and shed vortex

This velocity is calculated as sum of velocities induced by all of the line vortices that make horseshoe vortex $ABCD$. While circulation is constant along one horseshoe, and induced velocity is calculated by Biot-Savart law, it is possible to be written:

$$(\vec{w}_{i,j})_B = \frac{\Gamma_j}{4\pi} \left(\sum_{ABCD} \vec{G} \right)_{i,j}$$

where $\left(\sum_{ABCD} \vec{G} \right)_{i,j}$ is vector depending only on blade geometry, i.e. position of i -th control point and shape of j -th horseshoe vortex. Finally, we may obtain:

$$(\vec{w}_i)_B = \sum_{j=1}^n \frac{\Gamma_j}{4\pi} \left(\sum_{ABCD} \vec{G} \right)_{i,j}$$

On the similar way, it is possible to express other induced velocities as product of circulation and vector depending only of geometry:

$$(\vec{w}_i)_S = \frac{\Delta\tilde{\Gamma}}{4\pi} \vec{G}_S, \quad \text{and} \quad (\vec{w}_i)_W = \sum_{p=1}^M \frac{\Gamma_p}{4\pi} (\vec{G}_W)_p$$

According here developed vortex releasing method, $\Delta\tilde{\Gamma}$ can be expressed as:

$$\Delta\tilde{\Gamma} = \tilde{\Gamma}(t) - \tilde{\Gamma}(t - \Delta t) = \sum_{j=1}^n \Gamma_j(t) - \sum_{j=1}^n \Gamma_j(t - \Delta t)$$

By substituting above expressions for induced velocities in equation (8), and using necessary time notifications we may obtain:

$$\begin{aligned} \left(\sum_{j=1}^n \Gamma_j(t) \left(\sum_{ABCD} \vec{G} \right)_{i,j} \right) \vec{n}_i + \left(\sum_{j=1}^n \Gamma_j(t) - \sum_{j=1}^n \Gamma_j(t - \Delta t) \right) \vec{G}_S \cdot \vec{n}_i = \\ = 4\pi (\vec{V}_{Ti} - \vec{V}_\infty) \cdot \vec{n}_i - \left(\sum_{p=1}^M \Gamma_p (\vec{G}_W)_p \right) \cdot \vec{n}_i \end{aligned}$$

Circulation of bound vortices Γ_j are known from the calculations made in previous moment of time ($t - \Delta t$), so second term on the left side of equation above can be divided in known and unknown part at the time t .

Finally, the boundary condition for the i -th control point can be written as:

$$\sum_{j=1}^n a_{i,j} \Gamma_j(t) = b_i$$

where:

$$a_{i,j} = \left(\left(\sum_{ABCD} \vec{G} \right)_{i,j} + \vec{G}_S \right) \cdot \vec{n}_i$$

$$b_i = 4\pi (\vec{V}_T - \vec{V}_\infty) \cdot \vec{n}_i - \left(\sum_{p=1}^M \Gamma_p (\vec{G}_W)_p \right) \cdot \vec{n}_i$$

$$+ \left(\sum_{j=1}^n \Gamma_j(t - \Delta t) \right) \vec{G}_S \cdot \vec{n}_i$$

In this way, by writing equations for all control points, the equation set of the unknown bound circulations in the certain panel column at the time t is obtained.

Along with this equation set, the Kutta condition must be satisfied:

$$\sum_{j=1}^{n-1} \Gamma_j(t) + \Gamma_n(t) \left(1 + V_\infty \frac{\Delta t}{l_n} \right) = \sum_{j=1}^n \Gamma_j(t - \Delta t) \quad (9)$$

By adding the Kutta conditions to the equation set, an over-determined equation set is obtained.

Each blade consist of many cord-wise panel columns, and if we notate total number of them over all the blades as m , then total number of panels will be $n \cdot m$, as well must be number of boundary conditions of impermeability. Number of the Kutta conditions in the form (9) must be m . Thus, there are $n \cdot m + m$ equations, and $n \cdot m$ unknown bound circulations. Over-determined equation set, obtained in this way, can be reduced to the determined system by the method of least squares. After that, it can be solved by some of the usual approaches, by which the unknown values of circulations Γ_j at the time t are obtained.

5 DETERMINATION OF THE AERODYNAMIC FORCE

After unknown circulations are obtained, velocity at every point of the flow field is known, and we can use them for the determination of

aerodynamic forces that act on the blade. The calculation aerodynamic force is necessary for the defining of the blade position at the next moment of time. The total aerodynamic force is calculated as the sum of forces acting on all panels:

$$\vec{F} = \sum_{i=1}^N \vec{F}_i$$

Aerodynamic force acting on a single panel can be defined by introducing the Kutta condition in a vector form (Fig 6):

$$\vec{F}_i = \rho \vec{V}_\infty \times \Gamma_{i(e.f.)} \vec{BC}$$

where \vec{BC} is bound circulation vector and effective circulation can be defined by using:

$$\Gamma_{i(e.f.)} = \Gamma_i + \frac{1}{V_\infty} \frac{\partial}{\partial t} \int_{LE}^{M_j} \gamma dl$$

The integral should be calculated from the leading edge to the quarter-chord position of the i -th panel:

$$\Gamma_{i(e.f.)} = \Gamma_i + \frac{1}{V_\infty} \frac{\partial}{\partial t} \left(\sum_{k=1}^{i-1} \Gamma_k + \frac{\Gamma_i}{4} \right)$$

After determination of aerodynamic forces, moment of aerodynamic forces M_A , necessary for blade flapping equation, can be calculated as sum of moments acting on flapping hinge.

6 RESULTS AND DISCUSSION

Presented method for blade air-loads calculation has been implemented in a computer code. Forward flight application is presented for SA 341 "Gazelle" helicopter at moderate forward speed condition (advance ratio μ is 0.35). The rotor has three blades with constant NACA 0012 cross-sections, and the blade has a linear twist of $-6^\circ 20'$. In presented case, blade is modeled with 13 non-uniformly spanwise spaced panels (more panels at the tips), and 6 chordwise panels non-uniformly spaced (more panels near leading and trailing edges). Azimuthal step size of 10° and appropriate time discretization for calculations is used.

By analysing the drawings of the blade wakes (Figs. 7 and 8), it can be concluded that model applied in this paper gives reasonable simulation of actual wake behavior, specially in the domain of wake boundaries, where wake roll-up occurs (although it is slightly underestimated compared with existing experimental data). In

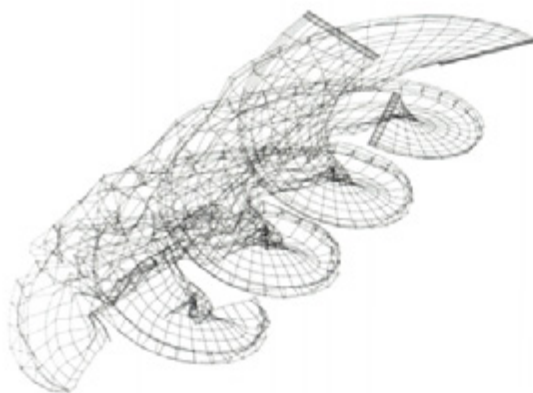


Fig. 7. Calculated free wake geometry; $\mu = 0.35$ (3D view)

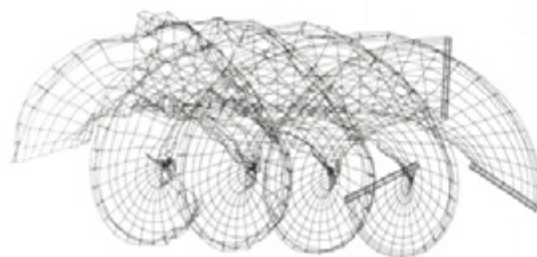


Fig. 8. Calculated free wake geometry; $\mu = 0.35$ (top view)

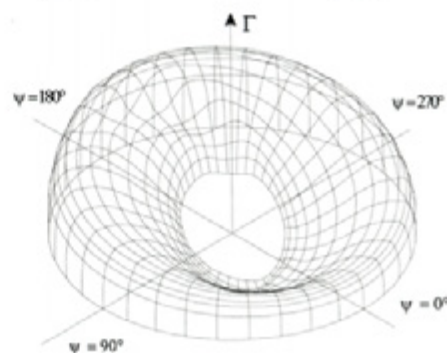
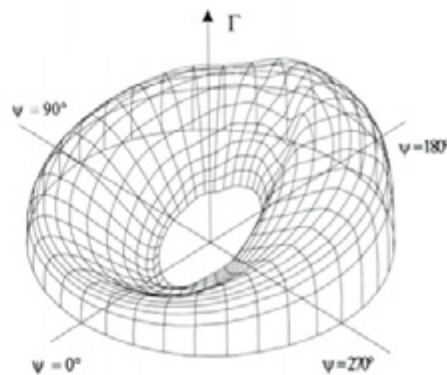


Fig. 9. Circulation distribution on the rotor disk; $\mu = 0.35$ (different points of view)

addition, larger wake distortion in the domains of the forerunning blades or their wakes is noticeable.

The program results (Figs. 9, 10 and 11), show the difference in circulation distributions at different azimuths, as well as the disturbances caused when blades are passing the wakes of other blades, and the characteristic reversal flow domains.

Range of azimuth where circulation is negative can be seen much clearly on the Figures 9 and 10.

Effects of the vortex-blade interaction are in the disturbing circulation and section lift distributions at the certain azimuth angles and span positions when blade passing the wakes of other blades. It is shown on the Figures 11 and 12.

On the Figure 13 is presented blade flapping angle distribution after achieving its periodical form.

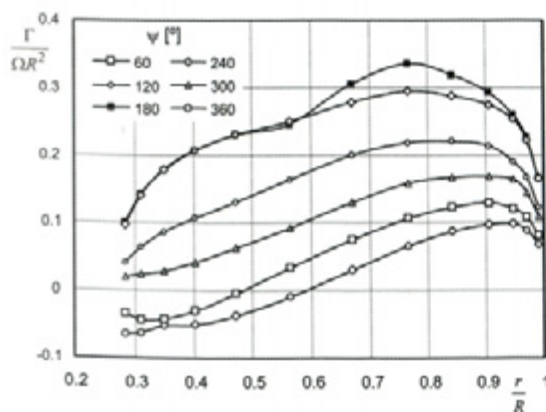


Fig. 10. Rotor blade spanwise circulation distribution at different azimuth positions; $\mu = 0.35$

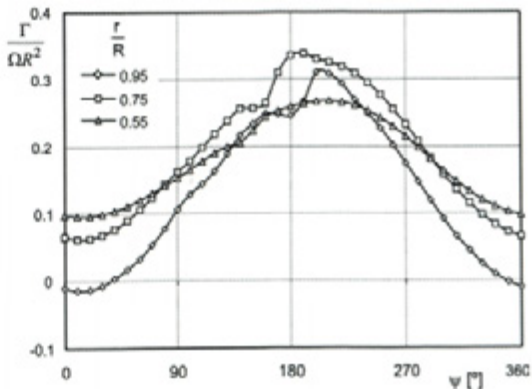


Fig. 11. Rotor blade azimuth circulation distribution at different radial positions; $\mu = 0.35$

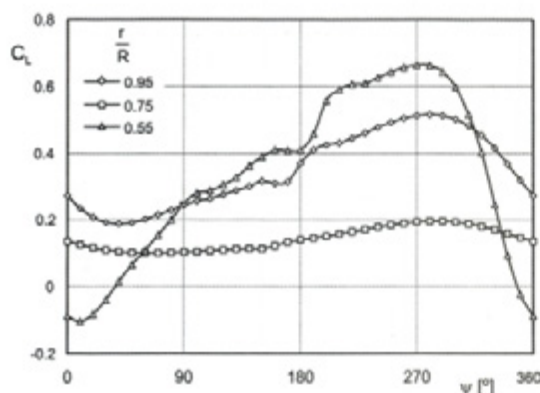


Fig. 12. Blade section lift coefficient azimuth distribution at different radial positions; $\mu = 0.35$

7 CONCLUSION

A solution for potential, incompressible helicopter main rotor flow field has been developed, and preliminary validations were done.

Obtained results can define suggestions for the future solution improvement. Firstly, by incorporating the transonic flow calculations, the advancing blade tip simulation would be more appropriate. Secondly, viscous interaction should be included as well, which would improve the wake roll-up simulation. The viscous vortex core simulation in time would improve the results concerning the wake vanishing effects far enough from the blade. Finally, introduction of the curvilinear vortex elements would give better results from the aspect of wake self-induction.

With these enhancements, this solution should prove to be a useful and efficient tool to the rotorcraft performance evaluation.

8 REFERENCES

- [1] Johnson, W. *Helicopter theory*. Princeton, New Jersey: Princeton University Press, 1980.
- [2] Johnson, W. Airloads and wake models for a comprehensive helicopter analysis. *Vertica*, 1990, vol. 14, no. 3, p. 225-300.
- [3] McCroskey, W. J. Some current research in unsteady fluid dynamics. *Journal of Fluids Engineering*, March 1977, p. 8-38.
- [4] Mello, O., Rand, O. Unsteady, frequency-domain analysis of helicopter non-rotating lifting surfaces. *Journal of the American Helicopter Society*, 1991, p. 70-81.
- [5] Chattot, J. J. *Calculation of three-dimensional unsteady transonic flows past helicopter blades*, NASA TP-1721, 1980.

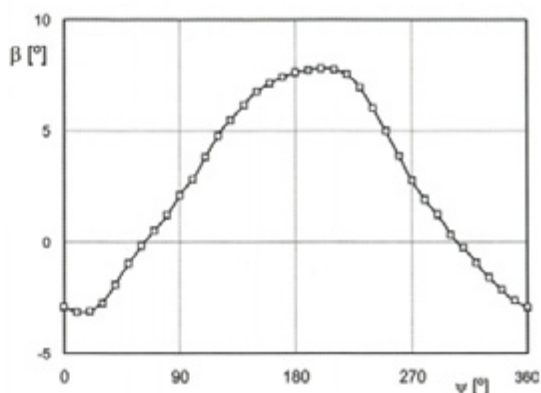


Fig. 13. Blade flapping angle; $\mu = 0.35$

- [6] Kießling, F. Computer aided derivation of equations of motion for rotary wing aeroelastic problems, *ICAS 1982*, ICAS Proceeding-82-2.1.3, p. 67-77.
- [7] Bramwell, A. R. S., Done, G., Balmford, D. *Bramwell's helicopter dynamics*, 2nd Ed. Oxford: Butterworth-Heinemann, 2001.
- [8] Colin, O. Unsteady thin - airfoil theory for subsonic flow. *AIAA Journal*, vol. 11, no. 2, 1973, p. 205-209.
- [9] Basu, B. C., Hancock, G. J. The unsteady motion of a two-dimensional aerofoil in incompressible inviscid flow. *Journal of Fluid Mechanics*, 1978, vol. 87, part 1, p. 159-178.
- [10] Sears, W. R. Unsteady motion of airfoils with boundary layer separation. *AIAA Journal*, vol. 14, no. 2, 1976, p. 216-220.
- [11] Ardonceau, P. Unsteady pressure distribution over a pitching airfoil. *AIAA Journal*, vol. 27, no. 5, 1989, p. 660-662.
- [12] Geissler, W. Nonlinear unsteady potential flow calculations for three-dimensional oscillating wings. *AIAA Journal*, vol. 16, no. 11, 1978, p. 1168-1174.
- [13] Katz, J., Plotkin, K. *Low-speed aerodynamics - from wing theory to panel methods*, Int. Ed., New York: McGraw-Hill, 1991.
- [14] Bliss D., Miller W. Efficient free wake calculations using analytical/numerical matching. *Journal of the American Helicopter Society*, 1993, pp. 43-52.
- [15] Torok M., Berezin, C. Aerodynamic and wake methodology evaluation using model UH-60A experimental data. *Journal of the American Helicopter Society*, 1994, p. 21-29.
- [16] Torok M., Chopra, I. A coupled rotor aeroelastic analysis utilising non-linear aerodynamics and refined wake modeling. *Vertica*, 1989, vol. 13, no. 2, p. 87-106.